



Communication

A Supramolecular Photosensitizer System Based on Nano-Cu/ZIF-8 Capped with Water-Soluble Pillar[6]arene and Methylene Blue Host–Guest Complexations

Chenhao Hu ^{1,†}, Yueyuan Yu ^{1,†}, Shuang Chao ¹, Huidan Zhu ², Yuxin Pei ¹, Lan Chen ^{2,*} and Zhichao Pei ^{1,*}

¹ Key Laboratory of Natural Products & Chemical Biology, College of Chemistry and Pharmacy, Northwest A&F University, Yangling 712100, China; huchenhao0620@163.com (C.H.); gongt118410@163.com (Y.Y.); chaoshuang@nwafu.edu.cn (S.C.); peiyx@nwafu.edu.cn (Y.P.)

² Center of College of Science & Technology, Hebei Agricultural University, Huanghua 061100, China; kyrazj1023@163.com

* Correspondence: chenlan19860303@126.com (L.C.); peizc@nwafu.edu.cn (Z.P.); Tel.: +86-3175605225 (L.C.); +86-2987091196 (Z.P.)

† These authors contributed equally to this work.

Abstract: Photodynamic therapy (PDT) as a safe, non-invasive modality for cancer therapy, in which the low oxygen and high glutathione in the tumor microenvironment reduces therapeutic efficiency. In order to overcome these problems, we prepared a supramolecular photosensitive system of O₂-Cu/ZIF-8@ZIF-8@WP6-MB (OCZWM), which was loaded with oxygen to increase the oxygen concentration in the tumor microenvironment, and the Cu²⁺ in the system reacted with glutathione (GSH) to reduce the GSH concentration to generate Cu⁺. It is worth noting that the generated Cu⁺ can produce the Fenton reaction, thus realizing the combination therapy of PDT and chemodynamic therapy (CDT) to achieve the purpose of significantly improving the anti-cancer efficiency.

Keywords: PDT; CDT; host–guest complexation; pillar[6]arene; combination therapy



Citation: Hu, C.; Yu, Y.; Chao, S.; Zhu, H.; Pei, Y.; Chen, L.; Pei, Z. A Supramolecular Photosensitizer System Based on Nano-Cu/ZIF-8 Capped with Water-Soluble Pillar[6]arene and Methylene Blue Host–Guest Complexations. *Molecules* **2021**, *26*, 3878. <https://doi.org/10.3390/molecules26133878>

Academic Editor: Feihe Huang

Received: 1 June 2021

Accepted: 22 June 2021

Published: 25 June 2021

Publisher's Note: MDPI stays neutral with regard to jurisdictional claims in published maps and institutional affiliations.



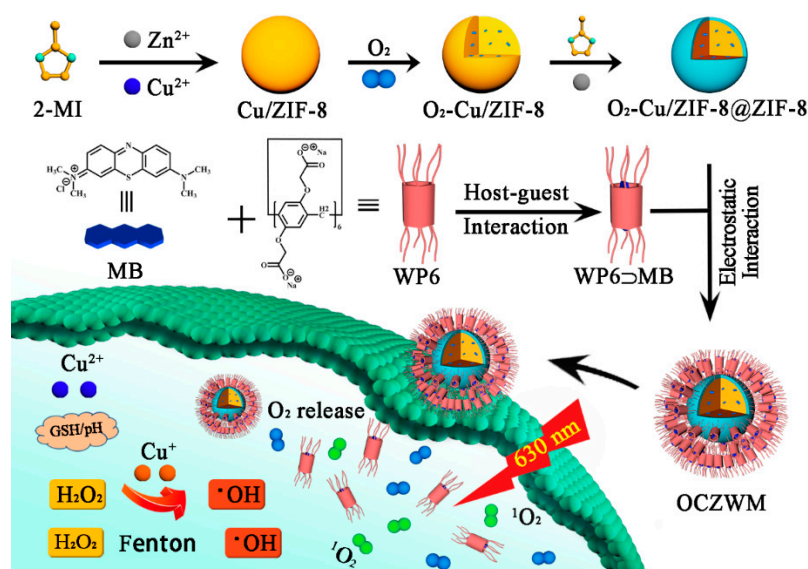
Copyright: © 2021 by the authors. Licensee MDPI, Basel, Switzerland. This article is an open access article distributed under the terms and conditions of the Creative Commons Attribution (CC BY) license (<https://creativecommons.org/licenses/by/4.0/>).

1. Introduction

As a safe and non-invasive method, PDT has been used in the treatment of numerous diseases. Especially in cancer treatment, PDT can not only reduce the recovery time of delicate surgical treatment, but also effectively kill drug- and radiation-resistant tumor cells, making it a new approach to replace traditional therapy [1,2]. As the core of PDT, photosensitizers (PSs) interact with oxygen molecules in tumor tissues under the stimulation of light to release reactive oxygen species (ROS), which can oxidize cell components and lead to cell necrosis and/or apoptosis [3–5]. However, low oxygen and high glutathione in the tumor microenvironment influences PSs to produce ROS, which leads to a reduction in the therapeutic efficiency [6–8]. In order to improve the problems encountered by PSS in PDT application, chemodynamic therapy (CDT), as a recent and emerging treatment method, produces hydroxyl radicals through the Fenton-like or Fenton reaction with hydrogen peroxide in cancer cells, and then triggers the apoptosis of cancer cells, which is often combined with PDT to improve therapeutic effect [9,10]. As a kind of synthetic hybrid materials, MOFs have shown great application potential in gas storage, chemical separation, catalysis, sensing, and drug delivery due to their high porosity [11,12]. In particular, supramolecular hybrid MOFs can not only effectively load PSs (to avoid dark toxicity, hydrophobicity, and photobleaching of the PSs), but also use metal ions in their structure to Fenton react with hydrogen peroxide in tumor cells [13,14].

Consequently, the development of a new supramolecular PSs-MOFs carriers to maintain or even improve the efficiency of PDT can not only overcome the photobleaching and dark toxic effects of PSs, but also the combination therapy of PDT and CDT can be achieved. Zeolitic imidazolate frameworks-8 (ZIF-8) is an important class of MOFs, which has great

potential in the construction of supramolecular drug delivery systems due to its stability in neutral, alkaline aqueous solutions and rapid decomposition in acidic solutions [15,16]. In addition, pillar[n]arenes, as a novel macrocyclic host molecule, can be used to construct nano-drug carriers through host-guest interaction [17,18], thus improving the solubility and stability of drugs [19–21]. Recently, based on the coordination between water-soluble carboxylated pillar[6]arene (WP6) and ZIF-8@DOX, we have developed a supramolecular targeted drug hybrid material with good dispersion efficiency, and host-guest complexation of WP6 and G as necessary modifiers to improve its water dispersion and give it target properties [22,23]. Herein, we design and synthesize Cu/ZIF-8@ZIF-8 nano carrier to adsorb O₂ and participate in a Fenton reaction with Cu²⁺ achieving CDT therapy. Thereafter, a supramolecular photosensitive system was prepared based on Cu/ZIF-8@ZIF-8 nano carriers capped with the host-guest complexation WP6-methylene blue (WP6-MB), while the WP6-MB complexations can prolong the ROS production time of MB under light irradiation, overcome photobleaching, and can also realize CDT/PDT combination therapy (see Scheme 1).



Scheme 1. Schematic of the construction of supramolecular photosensitizer system based on nano-Cu/ZIF-8@ZIF-8 capped with the host-guest complexation between WP6–MB.

2. Results and Discussion

WP6–MB host-guest complexation was synthesized according to the published procedure [22,24,25], which was fully characterized by ¹H NMR (Figures S1 and S2 in the Supporting Information). Cu/ZIF-8@ZIF-8 was first synthesized according to the published procedure [23,26]. The scanning electron microscopy (SEM) and transmission electron microscopy (TEM) showed that Cu/ZIF-8@ZIF-8 had typical hexagon morphology, with a diameter of approximately 190–290 nm (Figure 1a,b and Figure S4). In addition, TEM images showed that the obtaining Cu/ZIF-8@ZIF-8@WP6–MB had an obvious fuzzy edge compared with that of the obtaining Cu/ZIF-8@ZIF-8, which can be ascribed to the assembly of WP6–MB (Figure 1c). In order to further illustrate the homogeneity of ZIF materials in this design, we carried out an X-ray diffraction (Figure S4). The Cu/ZIF-8@ZIF-8@WP6–MB and MB UV-Vis spectra also demonstrated the WP6–MB capped Cu/ZIF-8@ZIF-8 through assembly (Figure 1d). In addition, the zeta potentials of OCZWM and ZIF were measured to prove the complexation of ZIF with WP6–MB (Figure S5). As the molar ratio of WP6 and MB is 1:1, and the mass ratio of WP6–MB and ZIF is 1:1, after calculation, it can be concluded that the loading rate of MB is 8.20% wt.

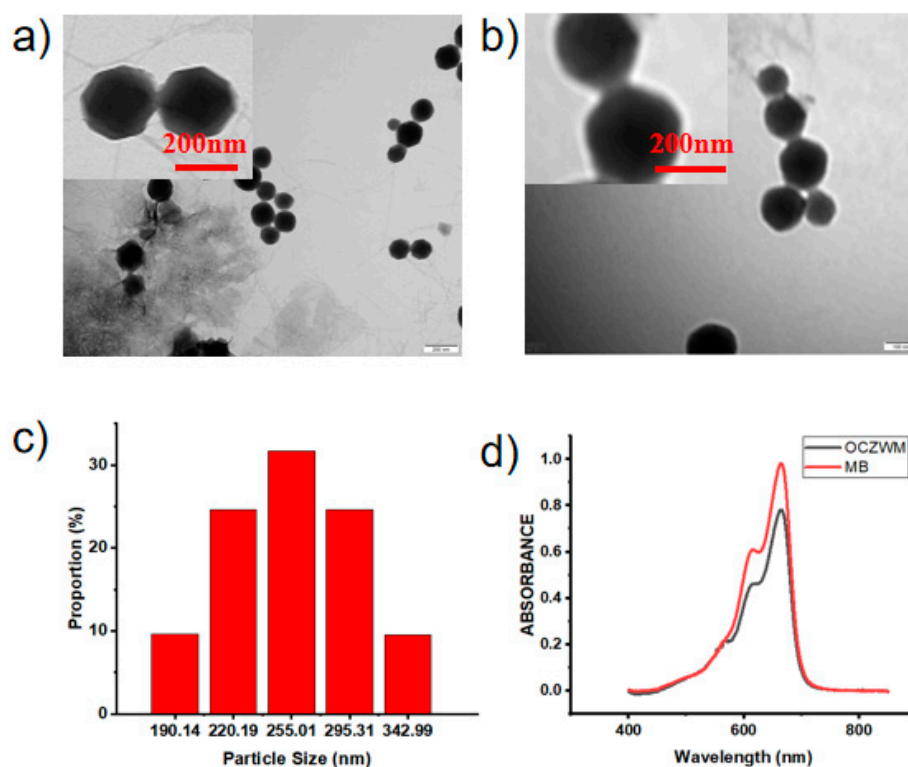


Figure 1. TEM images of (a) Cu/ZIF-8@ZIF-8 and (b) Cu/ZIF-8@ZIF-8@WP6-MB. The scale bar is 200 nm. Inset: partial enlarged images. The scale bar is 200 nm. (c) DLS data of Cu/ZIF-8@ZIF-8@WP6-MB. (d) UV-Vis spectra of Cu/ZIF-8@ZIF-8@WP6-MB and MB aqueous solution at room temperature.

To further demonstrate the loaded O_2 ability of Cu/ZIF-8@ZIF-8@WP6-MB, the O_2 content in the solution of OCZWM was measured under pH = 6.5 and pH = 7.4. As shown in Figure 2a, under acidic conditions, O_2 content in the OCZWM solution increased with time. However, under neutral conditions, there was no significant change in the O_2 content of the solution, indicating that the OCZWM had good O_2 loading and pH responsiveness. It is worth noting that the desorption properties of ZIF-8 in acidic environment led to the collapse of the system and the decomposition of oxygen, which is independent of the supramolecular structure. Then, we used an ROS probe to investigate the ROS content produced by the solution of OCZWM at 630 nm light irradiation under pH = 6.5 and pH = 7.4 (Figure 2b). The results show that the amount of ROS produced by OCZWM under neutral conditions is significantly lower than that under acidic conditions, which also verifies that the nanoparticles have good pH responsiveness. It also indicates that the O_2 released by nanoparticles in acidic environment can improve the production ROS by MB and the photosensitive efficiency. In addition, we utilized a GSH kit to detect the consumption of GSH by Cu^{2+} under pH = 6.5, pH = 7.4 conditions (Figure 2c). Obviously, due to the release of Cu^{2+} from the decomposition of nanoparticles in acidic solution, Cu^{2+} and GSH are reduced to form Cu^+ , resulting in a significant decrease in the concentration of GSH (see Figure 2c). It is worth noting that Cu^+ is more prone to the Fenton reaction than traditional Fe^{2+} under the acidic conditions, and its ability to produce $\cdot OH$ is stronger, which proves OCZWM to have a good CDT capacity.

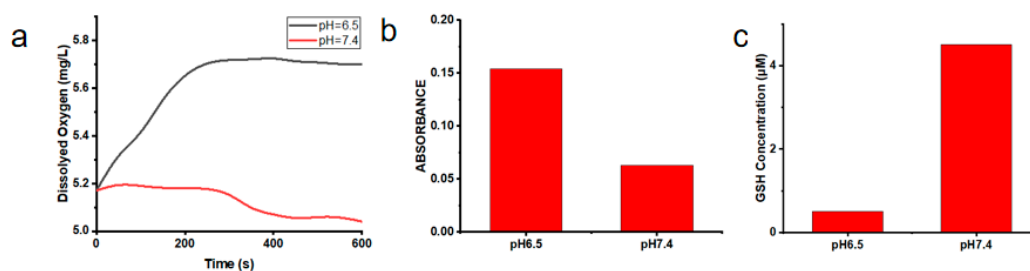


Figure 2. (a) the O_2 content under the solution of OCZWM in pH = 6.5 and pH = 7.4. (b) The amount of ROS produced by OCZWM in pH = 6.5 and pH = 7.4. (c) The GSH content under the solution of OCZWM in pH = 6.5 and pH = 7.4.

Next, we investigated the feasibility of OCZWM as a PDT/CDT nanocarrier in cells. Firstly, taking the HepG2 cells as models, the cell membrane permeability and cell internalization of OCZWM were detected by confocal laser scanning microscopy (CLSM) (Figure 3a). The results showed that significant red fluorescence appeared in the cytoplasm after 4 h. Thereafter, we incubated $10 \mu\text{m}$ OCZWM with HepG2 cells for 4 h, and compared with or without light irradiation for 40 min, using DCFH-DA as the probe molecule to determine the production of ROS in the cells. As shown in Figure 3b, it can be clearly observed that after light irradiation, green fluorescence of DCFH-DA can be produced, proving that OCZWM can be used in living cells.

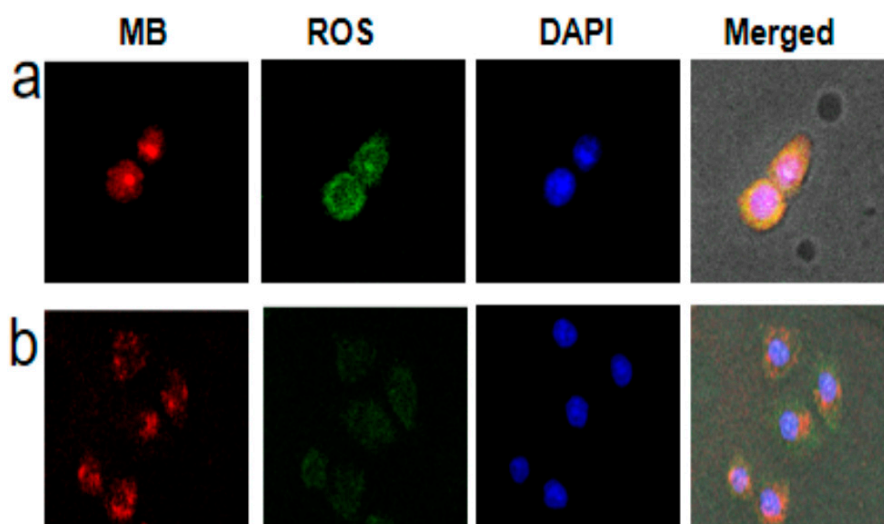


Figure 3. CLSM of HepG2 cells incubated with OCZWM (a) and Cu/ZIF-8@ZIF-8@WP6-MB (b). The scale bar is $50 \mu\text{m}$. (b) the GSH content under the OCZWM, Cu/ZIF-8@ZIF-8@WP6-MB, MB, control.

To gain further insight, the cell viability of OCZWM was carried out through MTT assay using HL7702 cells. As shown in Figure 4a, without light irradiation, OCZWM showed reduced dark toxicity compared to free MB with HL7702 cells. To provide further evidence of the anticancer attributes, the cell viability of OCZWM was carried out through MTT assay using HepG2 cells. Cu/ZIF-8@ZIF-8@WP6-MB were used as control groups. As shown in Figure 4b, under the condition of normal O_2 , the inhibition rates of OCZWM and Cu/ZIF-8@ZIF-8@WP6-MB on HepG2 cells were, in practical terms, the same. However, under the low O_2 condition, the inhibitory rate of OCZWM on HepG2 cells did not significantly change, while the inhibitory rate of Cu/ZIF-8@ZIF-8@WP6-MB on HepG2 cells significantly decreased. This indicates that the OCZWM is released O_2 in the tumor cells, improving the photodynamic therapy effect of MB. Moreover, it was found that, without light irradiation, the inhibition rates of OCZWM were higher than that of WP6-MB due to the CDT (Figure 4c).

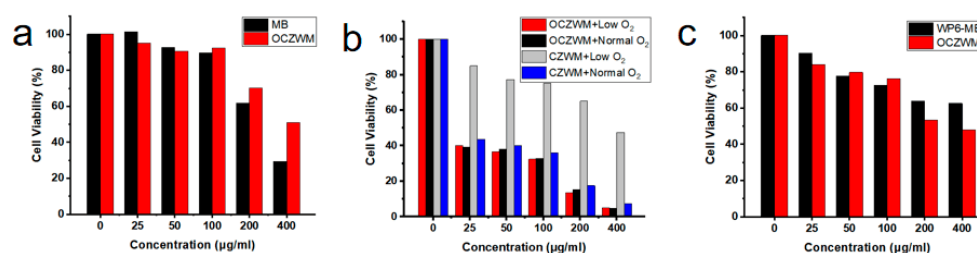


Figure 4. Relative cell viability of (a) HL7702 cells and (b) HepG2 cells after treatment with OCZWM, Cu/ZIF-8@ZIF-8@WP6-MB at different concentrations. (c) Relative cell viability of HepG2 cells after treatment with OCZWM, WP6-MB at different concentrations.

3. Materials and Methods

All reagents were purchased from commercial suppliers and used without further purification unless specified. Water used in this work was triple distilled. NMR spectra were recorded on a Avance neo 400 MHz Spectrometer, with working frequencies of 400 MHz for ¹H. Absorption spectra were collected by using a Shimadzu 1750 UV-visible spectrometer (Kyoto, Japan). Dynamic Light Scattering (DLS) data were obtained by Nano-2s ZEN3600. The confocal laser microscope (CLSM) data were acquired using a CLSM (Andor REVOLUTION WD). The power of light is 25 mW/cm² at 630 nm. TEM images were obtained from FEI TECNAI G2 SPIRIT BIO. SEM images were obtained from Nano SEM-450. Flow cytometry data were obtained from BD FACSAria™ III.

3.1. General Procedure for Cell Culture

HL7702 and HepG2 cells were cultured at 37 °C and 5% CO₂ in Dulbecco's modified Eagle's medium (DMEM, containing 10% fetal bovine serum (FBS) and 1% penicillin/streptomycin). The cells were fused with trypsin (0.5% *w/v* PBS) and separated. Cells were re-suspended in DMEM containing 10%FBS at a concentration of 1 × 10⁴ cells/mL.

3.2. Synthesis and Characterization of the Compounds WP6

WP6 was synthesized according to the literatures (S1–S3) and the ¹H NMR spectrum (see Figure S1). ¹H NMR (400 MHz, D₂O) δ 6.61 (s, 12H), 4.05 (s, 24H), and 3.84 (s, 12H).

3.3. General Procedure for OCZWM

Cu/ZIF-8 was synthesized according to the literatures [22]. The DLS and SEM of Cu/ZIF-8 were shown in Figures S3 and S4. The Cu/ZIF-8 prepared above was vacuum-dried to remove the methanol in the pores, and then was dispersed in methanol again for later use after being pumped with O₂ for 3 days. Then, ZIF-8 shells were uniformly grown around the Cu/ZIF-8 and the product (OCZ) was collected by centrifugation. Finally, WP6 assembled host-guest with MB in water (molar ratio 1:1) and the WP6-MB combined with OCZWM by coordination (mass ratio 1:1). The final products O₂-Cu/ZIF8@ZIF-8@WP6-MB (OCZWM) were obtained by centrifugation.

4. Conclusions

In conclusion, we successfully developed a novel supramolecular photosensitizer system based on nano-Cu/ZIF-8 capped with the water-soluble pillar[6]arene and methylene blue host-guest complexations. The resulting OCZWM possessed excellent O₂ load capacity and pH-sensitive release property. Flow cytometry and CLSM studies showed that OCZWM could be taken up by HepG2 cells and release MB efficiently. As a result, cell cytotoxicity measurements demonstrated that OCZWM in low O₂ exhibited good toxicity for hepatoma cancer cells. Furthermore, the *in vitro* evaluation of CDT tests towards HepG2 cells have shown that OCZWM can consume GSH and significantly improve the efficiency for PDT compared with that of WP6-MB. Therefore, this work provides a good

example of rational design of supramolecular photosensitizer system, which opens an efficient pathway for PDT/CDT combination therapy.

Supplementary Materials: The following are available online. Figure S1: ^1H NMR spectrum (400 MHz, D_2O) of WP6., Figure S2: ^1H NMR spectra (400 MHz, D_2O , 298 K): (a) WP6 (10.00 mM), (b) WP6:MB = 1:1; (c) MB (10.00 mM)., Figure S3: DLS data of Cu/ZIF-8., Figure S4: PXRD patterns of different materials, Figure S5: Zeta potential studies of OCZWM, Figure S6: SEM images of Cu/ZIF-8 (a), Cu/ZIF-8@ZIF-8. The scale bar is 2 μm .

Author Contributions: C.H. and Y.Y. conceived and designed the experiments, performed the majority of the experimental work, and wrote the manuscript; S.C. participated in developing the analytical method and the interpretation data; H.Z. performed part of the experimental work; Y.P. performed a small part of the experimental work; and Z.P. and L.C. supervised the work presented in this paper and revised the manuscript. All authors have read and agreed to the published version of the manuscript.

Funding: We thank National Natural Science Foundation of China (Nos. 21877088, 21772157 and 21572181), Hebei Agricultural University teacher-student collaboration (2021-BHXT-16) and Natural Science Foundation of Hebei Province (B2019204243) for financial support.

Institutional Review Board Statement: Not applicable.

Informed Consent Statement: Not applicable.

Data Availability Statement: The data presented in this study are available on request from the corresponding author.

Conflicts of Interest: The authors declare no conflict of interest.

Sample Availability: Samples of the compounds, carboxylated pillar[6]arene and the nanoparticles are available from the authors.

References

1. Lucky, S.S.; Soo, K.C.; Zhang, Y. Nanoparticles in Photodynamic Therapy. *Chem. Rev.* **2015**, *115*, 1990–2042. [[CrossRef](#)] [[PubMed](#)]
2. Dolmans, D.E.; Fukumura, D.; Jain, R.K. Photodynamic therapy for cancer. *Nat. Rev. Cancer* **2003**, *3*, 380–387. [[CrossRef](#)] [[PubMed](#)]
3. Couleaud, P.; Bechet, D.; Vanderesse, R.; Barberi-Heyob, M.; Faure, A.-C.; Roux, S.; Tillement, O.; Porhel, S.; Guillemin, F.; Frochet, C. Functionalized silica-based nanoparticles for photodynamic therapy. *Nanomedicine* **2011**, *6*, 995–1009. [[CrossRef](#)] [[PubMed](#)]
4. Kruger, C.A.; Abrahamse, H. Utilisation of Targeted Nanoparticle Photosensitiser Drug Delivery Systems for the Enhancement of Photodynamic Therapy. *Molecules* **2018**, *23*, 2628. [[CrossRef](#)] [[PubMed](#)]
5. Shao, C.; Shang, K.; Xu, H.; Zhang, Y.; Pei, Z.; Pei, Y. Facile fabrication of hypericin-entrapped glyconanoparticles for targeted photodynamic therapy. *Int. J. Nanomed.* **2018**, *13*, 4319–4331. [[CrossRef](#)]
6. Dang, J.; He, H.; Chen, D.; Yin, L. Manipulating tumor hypoxia toward enhanced photodynamic therapy (PDT). *Biomater. Sci.* **2017**, *5*, 1500–1511. [[CrossRef](#)]
7. Price, M.; Heilbrun, L.; Kessel, D. Effects of the oxygenation level on formation of different reactive oxygen species during photodynamic therapy. *Photochem. Photobiol.* **2012**, *89*, 683–686. [[CrossRef](#)]
8. LaRue, L.; Myrzakhmetov, B.; BEN Mihoub, A.; Moussaron, A.; Thomas, N.; Arnoux, P.; Baros, F.; Vanderesse, R.; Acherar, S.; Frochet, C. Fighting Hypoxia to Improve PDT. *Pharmaceuticals* **2019**, *12*, 163. [[CrossRef](#)] [[PubMed](#)]
9. Tang, Z.; Liu, Y.; He, M.; Bu, W. Chemodynamic Therapy: Tumour Microenvironment-Mediated Fenton and Fenton-like Reactions. *Angew. Chem. Int. Ed.* **2019**, *58*, 946–956. [[CrossRef](#)]
10. Lin, L.-S.; Huang, T.; Song, J.; Ou, X.-Y.; Wang, Z.; Deng, H.; Tian, R.; Liu, Y.; Wang, J.-F.; Liu, Y.; et al. Synthesis of Copper Peroxide Nanodots for H_2O_2 Self-Supplying Chemodynamic Therapy. *J. Am. Chem. Soc.* **2019**, *141*, 9937–9945. [[CrossRef](#)]
11. Zhang, C.C.; Wang, Y.; Phua, S.Z.F.; Lim, W.Q.; Zhao, Y.L. ZnO-DOX@ZIF-8 Core-Shell Nanoparticles for pH-Responsive Drug Delivery. *ACS Biomater. Sci. Eng.* **2017**, *3*, 2223–2229. [[CrossRef](#)]
12. Zheng, H.; Zhang, Y.; Liu, L.; Wan, W.; Guo, P.; Nyström, A.M.; Zou, X. One-pot Synthesis of Metal–Organic Frameworks with Encapsulated Target Molecules and Their Applications for Controlled Drug Delivery. *J. Am. Chem. Soc.* **2016**, *138*, 962–968. [[CrossRef](#)] [[PubMed](#)]
13. Wu, M.-X.; Gao, J.; Wang, F.; Yang, J.; Song, N.; Jin, X.; Mi, P.; Tian, J.; Luo, J.; Liang, F.; et al. Multistimuli Responsive Core-Shell Nanoplatfrom Constructed from Fe_3O_4 @MOF Equipped with Pillar[6]arene Nanovalves. *Small* **2018**, *14*, e1704440. [[CrossRef](#)]
14. Tan, L.-L.; Li, H.; Qiu, Y.-C.; Chen, D.-X.; Wang, X.; Pan, R.-Y.; Wang, Y.; Zhang, S.X.-A.; Wang, B.; Yang, Y.-W. Stimuli-responsive metal–organic frameworks gated by pillar[5]arene supramolecular switches. *Chem. Sci.* **2015**, *6*, 1640–1644. [[CrossRef](#)] [[PubMed](#)]

15. Zhang, H.; Jiang, W.; Liu, R.; Zhang, J.; Zhang, D.; Li, Z.; Luan, Y. Rational Design of Metal Organic Framework Nanocarrier-Based Codelivery System of Doxorubicin Hydrochloride/Verapamil Hydrochloride for Overcoming Multidrug Resistance with Efficient Targeted Cancer Therapy. *ACS Appl. Mater. Interfaces* **2016**, *9*, 19687–19697. [[CrossRef](#)] [[PubMed](#)]
16. Gao, L.; Chen, Q.; Gong, T.; Liu, J.; Li, C. Recent advancement of imidazolate framework (ZIF-8) based nanoformulations for synergistic tumor therapy. *Nanoscale* **2019**, *11*, 21030–21045. [[CrossRef](#)] [[PubMed](#)]
17. Chen, J.; Zhang, Y.; Zhao, L.; Chen, L.; Chai, Y.; Meng, Z.; Jia, X.; Meng, Q.; Li, C. Host-guest inclusion for enhancing anticancer activity of pemetrexed against lung carcinoma and decreasing cytotoxicity to normal cells. *Chin. Chem. Lett.* **2021**. [[CrossRef](#)]
18. Yang, K.; Pei, Y.; Wen, J.; Pei, Z. Recent advances in pillar[n]arenes: Synthesis and applications based on host–guest interactions. *Chem. Commun.* **2016**, *52*, 9316–9326. [[CrossRef](#)]
19. Duan, Q.P.; Cao, Y.; Li, Y.; Hu, X.Y.; Xiao, T.X.; Lin, C.; Pan, Y.; Wang, L.Y. pH-responsive supramolecular vesicles based on water-soluble pillar[6]arene and ferrocene derivative for drug delivery. *J. Am. Chem. Soc.* **2013**, *135*, 10542–10549. [[CrossRef](#)]
20. Chang, Y.; Yang, K.; Wei, P.; Huang, S.; Pei, Y.; Zhao, W.; Pei, Z. Cationic Vesicles Based on Amphiphilic Pillar[5]arene Capped with Ferrocenium: A Redox-Responsive System for Drug/siRNA Co-Delivery. *Angew. Chem. Int. Ed.* **2014**, *53*, 13126–13130. [[CrossRef](#)]
21. Xue, M.; Yang, Y.; Chi, X.; Zhang, Z.; Huang, F. Pillararenes, A New Class of Macrocycles for Supramolecular Chemistry. *Acc. Chem. Res.* **2012**, *45*, 1294–1308. [[CrossRef](#)] [[PubMed](#)]
22. Yang, K.; Yang, K.; Chao, S.; Wen, J.; Pei, Y.; Pei, Z. A supramolecular hybrid material constructed from pillar[6]arene-based host–guest complexation and ZIF-8 for targeted drug delivery. *Chem. Commun.* **2018**, *54*, 9817–9820. [[CrossRef](#)]
23. Yang, K.; Wen, J.; Chao, S.; Liu, J.; Yang, K.; Pei, Y.; Pei, Z. A supramolecular photosensitizer system based on the host–guest complexation between water-soluble pillar[6]arene and methylene blue for durable photodynamic therapy. *Chem. Commun.* **2018**, *54*, 5911–5914. [[CrossRef](#)] [[PubMed](#)]
24. Hu, X.-B.; Chen, Z.; Chen, L.; Zhang, L.; Hou, J.-L.; Li, Z.-T. Pillar[n]arenes (n = 8–10) with two cavities: Synthesis, structures and complexing properties. *Chem. Commun.* **2012**, *48*, 10999–11001. [[CrossRef](#)]
25. Shangguan, L.; Chen, Q.; Shi, B.; Huang, F. Enhancing the solubility and bioactivity of anticancer drug tamoxifen by water-soluble pillar[6]arene-based host–guest complexation. *Chem. Commun.* **2017**, *53*, 9749–9752. [[CrossRef](#)] [[PubMed](#)]
26. Dai, Y.; Xing, P.; Cui, X.; Li, Z.; Zhang, X.-M. Coexistence of Cu(ii) and Cu(i) in Cu ion-doped zeolitic imidazolate frameworks (ZIF-8) for the dehydrogenative coupling of silanes with alcohols. *Dalton Trans.* **2019**, *48*, 16562–16568. [[CrossRef](#)] [[PubMed](#)]